arXiv:cond-mat/0507192v1 [cond-mat.str-el] 7 Jul 2005

Dispersion of the high-energy phonon modes in $Nd_{1.85}Ce_{0.15}CuO_4$.

M. Braden,[1,*] L. Pintschovius,[2,3] T. Uefuji,[4] and K. Yamada[5]

[1] *II. Physikalisches Institut, Universität zu Köln, Zülpicher Str. 77, D-50937 Köln, Germany*
[2] *Forschungszentrum Karlsruhe, Institut fr Festkrperphysik, P.O.B. 3640, D-76021 Karlsruhe, Germany*
[3] *Laboratoire Léon Brillouin, CE Saclay, F-91191 Gif-sur-Yvette, France*
[4] *Institute for Chemical Research, Kyoto University, Uji 611-0011, Japan*
[5] *Institute of Materials Research, Tohoku University, Sendai 980-8577, Japan*

(Dated: February 2, 2008, **preprint**)

The dispersion of the high-energy phonon modes in the electron doped high-temperature superconductor $Nd_{1.85}Ce_{0.15}CuO_4$ has been studied by inelastic neutron scattering. The frequencies of phonon modes with Cu-O bond-stretching character drop abruptly when going from the Brillouin zone center along the [100]-direction; this dispersion is qualitatively similar to observations in the hole-doped cuprates. We also find a softening of the bond-stretching modes along the [110]-direction but which is weaker and exhibits a sinusoidal dispersion. The phonon anomalies are discussed in comparison to hole-doped cuprate superconductors and other metallic perovskites.

I. INTRODUCTION

The question about the role of electron phonon coupling in high-temperature superconductivity is still matter of controversy [1, 2, 3, 4, 5] and, most likely, will not be solved in the nearest future. Therefore, it appears interesting to continue to look for direct evidence for electron phonon coupling in these materials. In the conventional superconductors [6] signatures of strong electron phonon coupling can be found either in the form of dips in the phonon dispersion or by comparison with a non-superconducting reference material. In the case of the cuprates, however, there are no metallic non-superconducting reference materials; therefore, a safer way to discern electron-phonon coupling effects is to compare the phonon dispersion curves of cuprate superconductors to those of their insulating parent compounds. The latter approach is adopted in this study.

Very early, evidence for strong electron phonon coupling in the cuprate high-temperature superconductors was found in inelastic neutron scattering (INS) experiments on $La_{2-x}Sr_xCuO_4$ and $YBa_2Cu_3O_{6+\delta}$ [7]. The comparison of the phonon density of states (PDOS) measured on the insulating parent compounds, La_2CuO_4 and $YBa_2Cu_3O_6$, with that obtained on the optimally doped superconducting materials, $La_{1.85}Sr_{0.15}CuO_4$ and $YBa_2Cu_3O_7$, reveals a pronounced shift of spectral weight. Doping induces a frequency renormalisation of the modes with the highest energies which possess a longitudinal bond-stretching character, see Fig. 1. In contrast, the low and medium energy ranges in the PDOS exhibit less sensitivity to doping. More recently, similar effects were also reported for the electron doped superconducting cuprates [8, 9].

Studies of the phonon dispersion using single crystals and triple axis neutron spectrometry have clarified the shift of weight in the PDOS [10]. Along the [100] direction, the branches of the longitudinal bond-stretching character exhibit a softening when going from the zone-centre into the zone, for the polarization patterns of the bond-stretching modes see Fig. 1. Qualitatively, the dispersion is similar in $La_{1.85}Sr_{0.15}CuO_4$ [11, 12] and in $YBa_2Cu_3O_7$[13, 14, 15]. The branches are nearly flat close to the Brillouin zone centre, then show a steep decrease in frequency around $\mathbf{q}$=(0.25 0 0) and become flat again between (0.35 0 0) and (0.5 0 0). Along the [110] direction a nearly flat dispersion is observed in $La_{2-x}Sr_xCuO_4$ and in $YBa_2Cu_3O_7$, which still represents sizeable frequency renormalisation compared to the insulating parent compounds. The strong frequency renormalization of the zone-boundary modes is, however, not a particularity of the superconducting cuprates, but is seen in many doped perovskites : nickelates [16, 17], manganates [18] and superconducting $Ba_{1-x}K_xBiO_3$[19, 20, 21], the only metallic perovskite compound which does not exhibit the effect is superconducting Sr_2RuO_4[22].

We note that that the softening of the longitudinal bond-stretching phonons cannot be understood from phenomenological lattice dynamical models like the shell model. The insulator-to-metal transition upon doping entails a certain frequency reduction as a result of screening effects suppressing the LO-TO splitting of the polar modes at the Brillouin zone centre. However, in materials like the cuprates screening effects are confined to the long-wavelength phonons as it is illustrated in Fig. 2. Such behavior is indeed observed in the dispersion of the low-energy phonon branches with polar character in many oxide perovskites [16, 18, 19, 23].

Until recently the analysis of the bond-stretching phonon dispersion in the superconducting cuprates was restricted to $La_{2-x}Sr_xCuO_4$ and $YBa_2Cu_3O_{6+\delta}$, since only for these compounds it has been possible to grow single crystals of sufficient size for inelastic neutron scattering However, with the recent advance in synchrotron sources, inelastic x-ray scattering became more competitive and was applied to $Nd_{2-x}Ce_xCuO_4$ [24, 25], $HgBa_2CuO_4$[26] and very recently to $La_{2-x}Sr_xCuO_4$ [27].

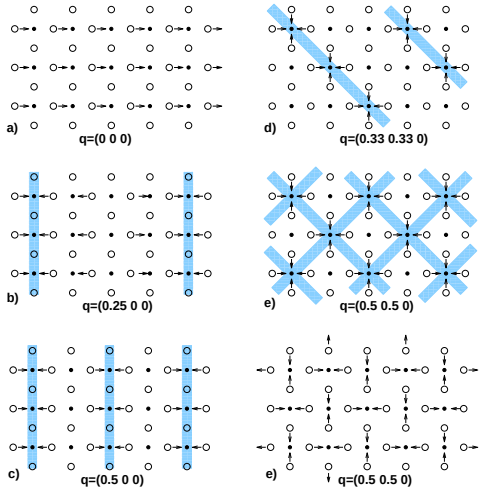

FIG. 1: Polarization patterns of the Cu-O bond-stretching phonon modes for different propagation vectors : the zone center mode (a), the longitudinal mode for **q**=(0.25,0,0) (b), the linear or half-breathing mode (c), the longitudinal mode for **q**=(0.33,0.33,0) (d), the planar breathing mode (e), and the quadrupolar mode of transverse character at **q**=(0.5,0.5,0).

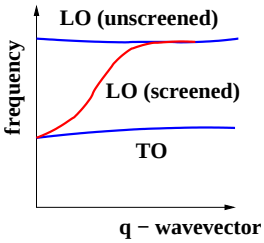

FIG. 2: Illustration of the screening of polar modes in a metal with low carrier concentration, when the electronic susceptibility is described in a free electron model.

For $HgBa_2CuO_4$ Uchiyama et al. [26] find a dispersion similar to that observed in $YBa_2Cu_3O_7$ [13, 14], i.e. the same step-like downwards dispersion in the bond-stretching branch along [100]. In the electron-doped material $Nd_{2-x}Ce_xCuO_4$ the high-energy dispersion is more complex since there is another longitudinal branch of the same symmetry which interacts with the bond-stretching branch, see below. d'Astuto et al. [24, 25] report that the frequencies of the modes with Cu-O bond-stretching character drop near **q**∼(0.2 0 0) falling below those of an other branch. However, the intensity related to bond-stretching character could not safely be followed beyond (0.15 0 0) in the inelastic x-ray scattering experiment. This motivated us to investigate the high-energy phonon dispersion in $Nd_{1.85}Ce_{0.15}CuO_4$ by inelastic neutron scattering after large superconducting single crystals of this material became finally available.

The paper is organized as follows: the next Section describes our experimental technique. Thereafter, we explain the phenomenological model used to analyze the data. Then, we present results for the [100] direction and the [110] direction and discuss the polarization patterns of the different phonon branches. Finally, we compare the phonon anomalies found in $Nd_{2-x}Ce_xCuO_4$ to those observed in hole-doped cuprates and also to those observed in other metallic oxide perovskite materials.

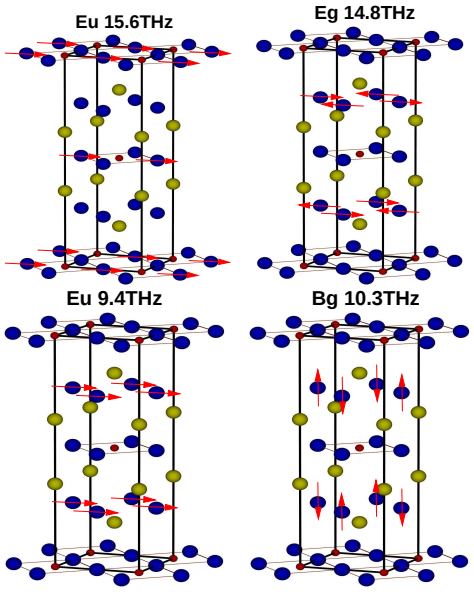

FIG. 3: Polarization patterns of the zone-center modes relevant for the Δ_1 high-energy dispersion. Large blue balls correspond to oxygen atom, small red balls to Cu atoms and the large yellow ones to Nd/Ce-sites.

II. EXPERIMENTAL

Two single crystals of $Nd_{1.85}Ce_{0.15}CuO_4$ were grown by a floating zone technique using a mirror furnace at Kyoto University. The crystals exhibit the superconducting transition at 25 K and samples obtained with this method were already used in many studies [28, 29]. Inelastic neutron scattering experiments were performed on the 1T spectrometer at the Orphée reactor using Cu(111) and Cu(220) monochromators and a pyrolithic graphite (002) analyzer. Higher order contaminations were suppressed with a pyrolithic graphite filter in front of the analyzer. Double focusing was applied on the monochromator and on the analyzer sides. Two single crystals, each of about 500mm^3 volume, were co-aligned in the [100]/[010] scattering geometry and cooled in a closed He-cycle cryostate. An additional experiment was performed with one crystal in the [100]/[001] orientation.

III. RESULTS AND DISCUSSION

The polarization patterns of the Cu-O plane-polarized bond-stretching modes are depicted in Fig. 1. For the longitudinal modes at the zone-boundaries there is an alternation of Cu-sites with short and long metal-oxygen distances and therefore, the modes at (0.5,0,0) and (0,5,0,5,0) are called half-breathing and breathing modes, respectively. These modes may strongly couple to the charges, since smaller metal-oxygen distances point to a higher metal valence [30]. Fig. 1 depicts also the polarization patterns of some other plane-polarized Cu-O1 bond-stretching modes whith a regard to discussion which modes can be expected to couple strongly to charge fluctuations. To this end, loci of dynamical charge accumulation favored by the atomic displacements are highlighted.

III.1 Phenomenological model

The above mentioned anti-crossing phenomena - which are absent in the case of $La_{2-x}Sr_xCuO_4$ because of a different structure - makes the use of a lattice dynamics model indispensable to correctly assign the various high-energy phonon modes in $Nd_{2-x}Ce_xCuO_4$. This interaction of the longitudinal optical branches has been seen in the x-ray studies [24, 25] and is predicted by calculations with the phenomenological model. The complication arises from the shift of the second oxygen site (O1 labels the in-plane oxygen and O2 the out-of-plane one) from the apical position at (0 0 0.17) in $La_{2-x}Sr_xCuO_4$ to (0.25 0.25 0.25) in $Nd_{2-x}Ce_xCuO_4$ [31], where it is stronger bonded with the RE-ions. In consequence, the vibrations of O2 parallel to the CuO_2-planes exhibit higher energies and may interact with the Cu-O bond-stretching modes in $Nd_{2-x}Ce_xCuO_4$. In order to put the assignment of the various high-energy modes onto firm ground, we measured the dispersion of all high-energy branches of a particular symmetry and compared the measured scattering intensities with the model predictions. Since it was beyond the scope of our experiments to determine a full set of dispersion curves we did not develop a new model but adapted the one fitted to the phonon dispersion of the parent compound Nd_2CuO_4 which is described in reference [32]. Only a few changes were necessary in order to achieve a satisfying agreement with the experimentally obtained dispersion. The model parameters are given in Table II, the crystal structure data were taken from reference [31]. We use a shell model [33] with Born-Mayer potentials describing the repulsive interactions. The shell charges of Nd and Cu and the amplitude of the O-O Born-Mayer potential were slightly adapted. Further, we included a longitudinal force constant between Cu and the O2-oxygen as was done for the non-doped compound [32] to arrive at a fully satisfactory description of the experimental dispersion curves.

ionic part				potentials			
ion	Z	Y	K	pair	A(eV)	r_0 (Å)	C (eV/Å^6)
Cu	1.64	1.4	2.0	Nd-O	2000	0.319	-
Nd	2.30	-4.9	8.0	Cu-O	3950	0.228	-
O1	-1.56	-3.0	2.0	O-O	2650	0.284	-100
O2	-1.56	-3.0	2.0				

force constants (dyn/cm)	
pair	F
Cu-O2 (long.)	13372
lin.-breathing	93800
plan.-breathing	69300

TABLE I: Lattice dynamics model parameters for the description of the phonon dispersion in $Nd_{1.85}Ce_{0.15}CuO_4$; for the explanation of the parameters see text; Z,Y are given in electron charges; K in 10^6dyn/cm.

The main lattice dynamical difference between the parent and the doped compounds concerns the screening of the Coulomb-interaction through the free charge carriers. We describe the electronic susceptibility by the Lindhard-function for a free electron gas taking exchange corrections into account. Such model invariably produces complete screening at long distances, which means that the splitting between longitudinal optic (LO) and transverse optic (TO) phonon frequencies will disappear at the zone center. However, when passing into the zone, the screening has to occur at smaller distances where it will be less effective and the LO-TO splitting may partially recover yielding an increasing dispersion. This scenario describes perfectly the dispersion of phonon branches with polar character at intermediate energies in many doped perovskites [16, 18, 19, 23]. In particular, it applies to the modes with the strongest polar character which are the bond-bending modes related to ferroelectricity.

In the case of $Nd_{2-x}Ce_xCuO_4$ we obtain a screening vector of $k_s = 0.42$Å^{-1} in good agreement with the analysis of the inelastic x-ray scattering results [24]. The screening-vector is furthermore comparable to the one found in $La_{2-x}Sr_xCuO_4$, $k_s = 0.39$Å^{-1} for x$\sim$0.1 [32]. In view of the higher doping in our sample the screening in the electron doped system appears to be somewhat less effective than in the hole-doped compounds. However, in our analysis the screening is mainly determined by the slope of the O2-branch. Therefore, we cannot exclude that the screening is somewhat more effective in the Cu-O plane.

As has been pointed out in the introduction, screening treated within the free electron model is unable to explain the downward dispersion of the longitudinal branches along the [100] and the [110] directions. In order to reproduce such a behavior - which is sometimes called over-screening - we included additional force constants lowering the frequencies of the Cu-O1 bond-stretching

modes at the zone boundary in the [100] (linear breathing term) or in the [110] direction (planar breathing term), respectively. The linear and planar breathing constants (see Table I) correspond to force constants between a particular O1-site and the other O1's connected with the same Cu-atom. A displacement of the first O1 towards the Cu-site results in forces on the other O1's also directed towards the Cu-site. With the linear and planar breathing constant, the forces act on just the opposite and on all three surrounding O1's, respectively. With these parameters a quantitative description of the dispersion is achieved [34]. We note that such terms have been used previously to describe the phonon anomalies in hole-doped compounds (see, e.g., [15]).

The softening of the zone-boundary modes observed in the superconducting cuprates can be considered as being due to an over-screening of the Coulomb-potentials requiring a special electronic susceptibility [35, 36]. Assuming that charges may fluctuate between different cation-sites on the frequency scale of the phonon modes one may explain the softening of the breathing modes [4, 35, 36]. Ab initio calculations of the phonon dispersion for the hypothetic material $CaCuO_2$ [37] and for $YBa_2Cu_3O_7$ [38] agree with the soft half-breathing mode frequency rather well, but they also obtain a soft breathing mode at **q**=(0.5 0.5 0) and they do not find the step-like dispersion [37, 38]. Although the breathing force constants in our model do not posses a clear physical meaning they appear to mimic the particular electronic susceptibility in the metallic cuprates [34].

Table II resumes the group theoretical analysis. The zone center modes can be separated according to the irreducible representations, whose the polarization patterns are given in Table II. Along the [100] (Δ) and along the [110] direction (Σ), modes split into four different representations, all compatibility relations are given in Table II.

	Nd	Nd'	Cu	O1	O1'	O2	O2'
	0 0 .35	0 0 -.35	0 0 0	.5 0 0	0 .5 0	.5 0 .25	0 .5 .25
1 B_g	0 0 0	0 0 0	0 0 0	0 0 0	0 0 0	0 0 A	0 0 -A
1 B_u	0 0 0	0 0 0	0 0 0	0 0 A	0 0 -A	0 0 0	0 0 0
1 A_g	0 0 A	0 0 -A	0 0 0	0 0 0	0 0 0	0 0 0	0 0 0
4 A_u	0 0 A	0 0 A	0 0 B	0 0 C	0 0 C	0 0 D	0 0 D
2 E_g	A 0 0	-A 0 0	0 0 0	0 0 0	0 0 0	B 0 0	-B 0 0
5 E_u	A 0 0	A 0 0	B 0 0	C 0 0	C 0 0	D 0 0	D 0 0
7 Δ_1	A 0 B	A 0 -B	C 0 0	D 0 0	E 0 0	F 0 G	F 0 -G
2 Δ_2	0 A 0	0 -A 0	0 0 0	0 0 0	0 0 0	0 B 0	0 -B 0
5 Δ_3	0 A 0	0 A 0	0 B 0	0 C 0	0 D 0	0 E 0	0 E 0
7 Δ_4	A 0 B	-A 0 B	0 0 C	0 0 D	0 0 E	F 0 G	-F 0 G
6 Σ_1	A A B	A A -B	C C 0	D E 0	E D 0	F F 0	F F 0
3 Σ_2	A -A 0	-A A 0	0 0 0	0 0 B	0 0 -B	C C 0	-C -C 0
6 Σ_3	A -A 0	A -A 0	B -B 0	C D 0	-D -C 0	E -E F	E -E -F
6 Σ_4	A A B	-A -A B	0 0 C	0 0 D	0 0 D	E -E F	-E E F

7 Δ_1 : 5 E_u + 1 A_g + 1 B_g	5 Δ_3 : 5 E_u
2 Δ_2 : 2 E_g	7 Δ_4 : 3 E_g + 4 A_u + B_u
6 Σ_1 : 5 E_u + 1 A_g	6 Σ_3 : 5 E_u + B_g
3 Σ_2 : 2 E_g + B_u	6 Σ_4 : 4 A_u + 2 E_g

TABLE II: Upper part :Polarization schemes according to the crystal structure of $Nd_{2-x}Ce_xCuO_4$ for all Γ-modes and for the representations along the [100] and [110] directions (labeled Δ and Σ respectively); the first line gives the positions of 7 atoms forming a primitive unit, the following lines show the displacements of these atoms. A letter at the i-position, signifies that this atom is moving along the i-direction, a second appearance of the same letter signifies that the second atom moves with the same amplitude ("-" denotes a phase shift) in the corresponding direction. Lower part : compatibility relations along the [100] and [110] directions

III.2 Phonon dispersion in [100] direction

In the [100] direction the branches corresponding to the Δ_1-representation start from the E_u-, A_g- and B_g-modes at the zone center. The polarization patterns of the four modes with the highest energies are shown in Fig. 3. The patterns were calculated with the lattice dynamical model fitted to the measured dispersion, see above. In addition to the CuO1 bond-stretching mode (E_u) at the highest energy, there is the CuO1 bond-bending mode (E_u) at about 10THz, the B_g-mode at 10.3 THz and the O2-mode (E_u) at 9.4 THz. The B_g-mode corresponds to a motion of O2 parallel to the c-axis; its frequency is observed by Raman-scattering at 10.0–10.3 THz [39, 40, 41]. E_u-modes are Infra-Red active; however, the reported measurements are not conclusive, possibly due to insufficient sample quality [41, 42]. Fig. 3 shows also the displacement pattern of the highest E_g mode. This mode is the starting point of a branch with Δ_4 symmetry which lies in the same frequency range as those associated with the Cu-O1 respectively Nd-O2 bond-stretching vibrations. Measurements aiming at the dispersion of the latter branches were performed in Brillouin zones with zero structure factor for the Δ_4-modes.

Energy scans at Q-values with favorable structure factors for Cu-O1-bond-stretching phonons are shown in Fig. 4. Results are shown both for medium and high resolution set-ups. At the zone center, (3 1 0), the bond-stretching mode can be easily detected. For intermediate **q**-values, however, it is obscured by the strong signal of the Nd-O2 vibrations, whose frequency rapidly increases with q whereas frequencies associated with the Cu-O1-bond-stretching vibrations abruptly decrease. The steep frequency increase in the O2-branch and the frequency decrease of the bond-stretching modes render the measurement very sensitive to the resolution conditions. At **Q**=(3.15 0 0) the increasing branch is focused and at **Q**=(2.85 0 0) the decreasing one, see Fig. 4. The interaction of the O1 and the O2-branch occurs around **q**=(0.2 0 0). At **q**=(0.3 0 0) the energy of the Cu-O1-bond-stretching mode is already more than 2 THz below that of the O2-mode. In addition, the Cu-O1-bond-stretching

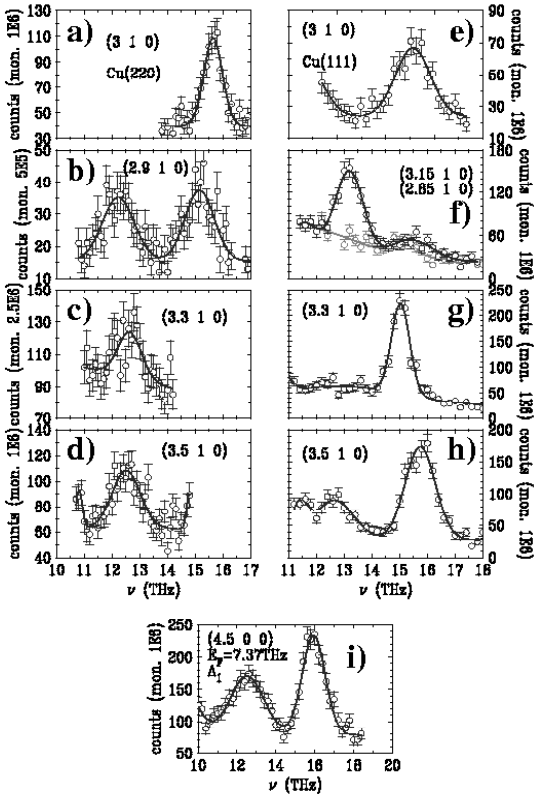

FIG. 4: Scans across the longitudinal bond-stretching modes with Δ_1-symmetry: a)-d) are obtained with high resolution conditions (Cu(220) monochromator), e)-h) with medium resolution (Cu(111)-monochromator) and i) with low resolution (Cu(111)-monochromator with a final energy of 7.37 THz) . Lines correspond to fits with Gaussians.

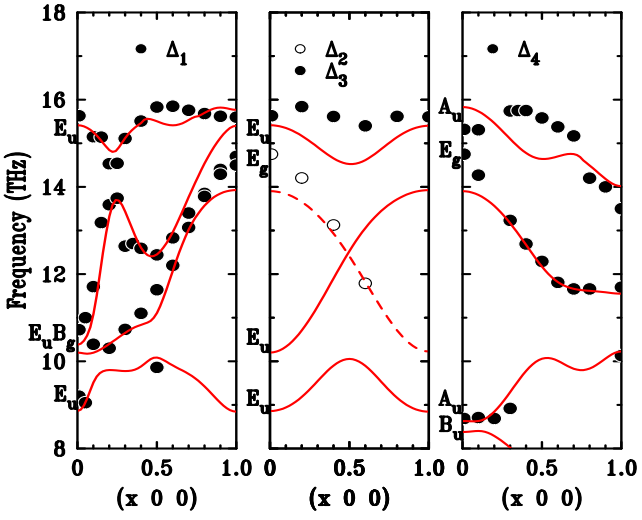

FIG. 5: Dispersion of the high-energy phonon branches in $Nd_{1.85}Ce_{0.15}CuO_4$ in [100] direction. Symbols denote the experimental data and lines frequencies calculated with the phenomenological model.

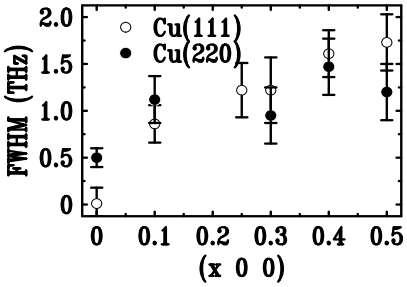

FIG. 6: Resolution corrected linewidths observed for plane-polarized bond-stretching modes in $Nd_{1.85}Ce_{0.15}CuO_4$ in the [100] direction at T = 10 K.

mode is broadened. Therefore, it has a stronger weight in the lower resolution configuration. At **q**=(0.5 0 0) the bond-stretching mode is clearly observed at 12.5 THz. The dispersion of the Δ_1-modes is resumed in Fig. 5.

We find a strong broadening of the Cu-O1-bond-stretching modes for **q**-values in the Brillouin-zone. The full widths at half maximum were obtained by fitting Gaussian profiles to the scans and by correcting for the resolution, see Fig. 6. Note that the experimental resolution for measurements with the Cu(220) monochromator is much smaller (0.6 THz) than the width of the observed phonon peak. In spite of the difficulties to separate Cu-O bond-stretching modes from other ones our data unambiguously shows that these modes are significantly broadened, yielding another evidence for strong electron phonon coupling in $Nd_{2-x}Ce_xCuO_4$.

Due to the body centered stacking of the CuO_2-planes in $Nd_{2-x}Ce_xCuO_4$, the reciprocal lattice vector **Z**=(1 0 0) is not a Brillouin-zone centre but a zone boundary: the corresponding modes are characterized by a phase shift of the displacements of atoms at **r**=(0 0 0) and at (0.5 0.5 0.5). Therefore, the displacement patterns of the modes at the zone center and of those at **Z** just differ by a phase shift in neighboring CuO_2 planes. For the bond-stretching modes, one may expect similar phonon frequencies at Γ and at **Z** due to the weakness of the inter-plane couplings involved. Following the Cu-O1 bond-stretching signal beyond (0.5 0 0) we indeed find the expected frequency increase. However, between (0.6 0 0) and (1 0 0) there is an interaction with another branch. The Δ_1-branch starting at the B_g-mode exhibits an increasing dispersion. Beyond **q**=(0.6 0 0) these modes strongly mix with the Cu-O1-bond-stretching ones. The high-energy phonon dispersion obtained by measurements in different Brillouin-zones, including zones with a large $\mathbf{Q}_l$ component, are resumed in Fig. 5. Only a few measurements were made in the low energy region because we did not expect strong doping-induced changes here. The zone center modes in the range 8.5 to 10.5 THz were investigated in some detail because there is a strong interaction between Δ_1 branches of

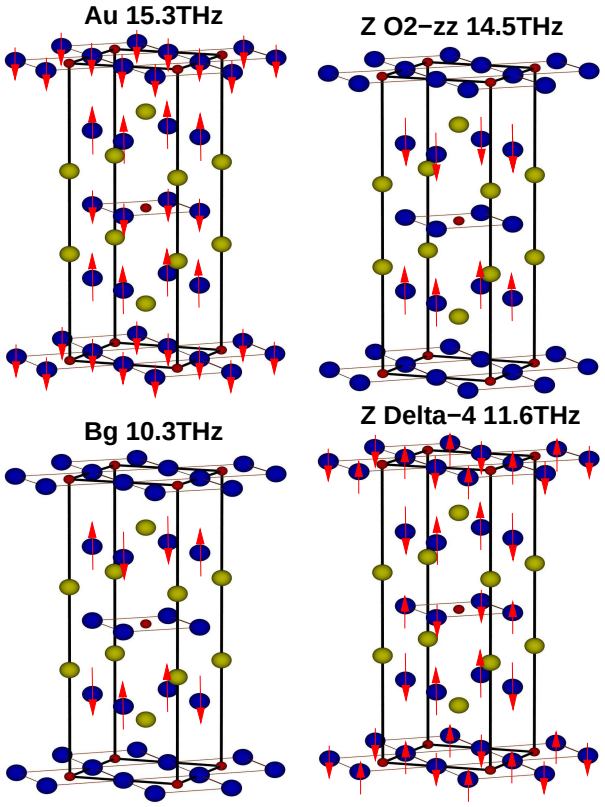

FIG. 7: Polarization patterns of zone-center and **Z**-point modes with strong polarization along the c-direction. Large blue balls correspond to oxygen atom, small red balls to Cu atoms and the large yellow ones to Nd/Ce-sites.

different polarization starting from these modes. These interactions virtually vanish, however, for $\mathbf{q}> 0.1$ because the dispersion of the interacting modes is very different.

We now turn to the c-polarized high-energy modes. Their polarization patterns are shown in Fig. 7: at the zone center, there is an A_u-mode near 15 THz and the B_g-mode at 10.3 THz already mentioned. The O2-atoms exhibit a polarization along the c direction in both modes, but the modes differ with respect to the phase between neighboring O2-sites. In the A_u-mode, all O2's move in phase, whereas they move out of phase in the B_g-mode, see Fig. 7. At the **Z**-point, too, there are two c-polarized O2-modes corresponding to the in-phase and out-of-phase movement of the O2-ions at the same z-level. The B_g mode is connected through the Δ_1-branches with the in-phase movement at higher frequency; note that there are some interactions with other branches. The A_u-mode connects with the in-phase **Z**-mode through the Δ_4-branches. Typical scans aiming at the frequencies of these phonon modes are shown in Fig. 8. Compared to the longitudinal plane-polarized modes these phonons are better defined, i.e. their line-widths are smaller. The in-phase Δ_1-mode at **Z** is of special interest since all O2-sites move in-phase, which means

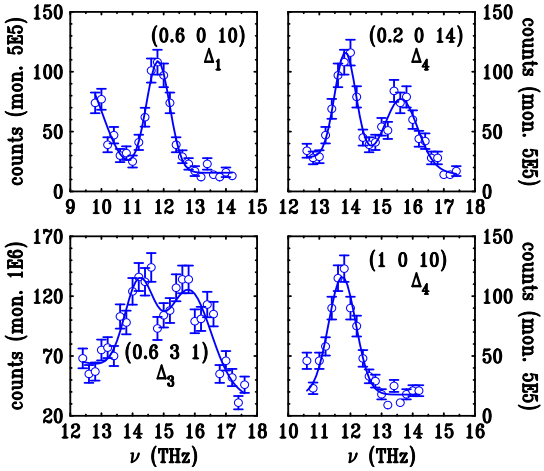

FIG. 8: Several scans across high-energy phonons with different characters as indicated in the labels. Symbols denote the raw intensities and lines correspond to fits with Gaussians.

that all neighboring O2's of a particular CuO_2-layer come closer at the same time, see Fig. 7 . Therefore, this O2-vibration may induce strong charge fluctuations between the CuO_2 planes; it is related in character with the half-breathing mode, and one might expect a strong coupling with an inter-layer charge modulation. The corresponding mode in $La_{1.85}Sr_{0.15}CuO_4$, labeled O_{ZZ}, indeed is rather anomalous with a large line width and a frequency renormalisation compared to the parent compound by several THz [10]. This effect is interpreted by Falter et al. [4] as due to strong coupling with the inter-layer plasmon mode. We find that the O_{ZZ}-mode is not well defined in $Nd_{1.85}Ce_{0.15}CuO_4$ as well indicating a large intrinsic line width. Unfortunately, it is difficult to isolate the contributions of the c-polarized Z-point phonon from those with the in-plane polarization , but the observation of a three-peak structure obtained at several **Z**-points clearly proves that the c-polarized mode exhibits a high energy. There is strong evidence that the O_{ZZ}-mode has a large line width. Compared to $La_{1.85}Sr_{0.15}CuO_4$ the O_{ZZ}-mode in $Nd_{1.85}Ce_{0.15}CuO_4$ appears to be less anomalous.

III.2 Phonon dispersion in [110] direction

The phonon dispersion in the [110] direction, Σ, was studied, again with the focus on the bond-stretching branches. Typical scans are shown in Fig. 9, and the phonon dispersion derived from the data is drawn in Fig. 10. Again, the analysis is complicated by the interaction of the Cu-O1 with the Nd-O2 bond-stretching branches. The scattering associated with the latter modes is in most configurations dominant. Nevertheless, we were able to unambigously determine the dispersion of the branches of interest. The following picture emerged: the branch

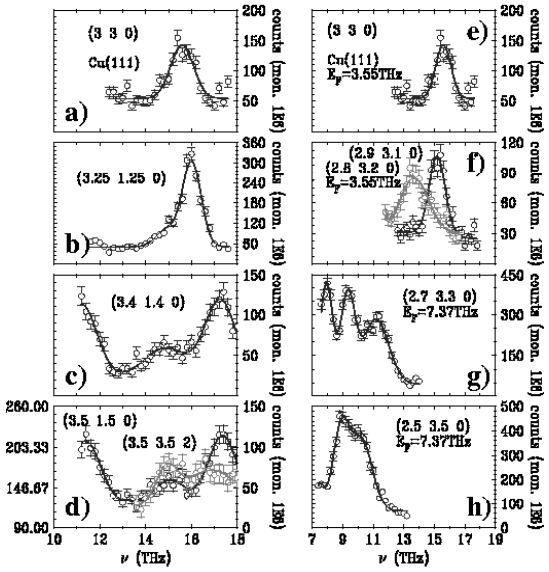

FIG. 9: Scans across the longitudinal a-d) and transverse e-h) bond-stretching modes with Σ_1 and Σ_3 symmetry, respectively. All scans were performed using a Cu(111) monochromator with a final energy of E_f=3.55 THz, except that in g) and h) where E_f=7.37 THz. .

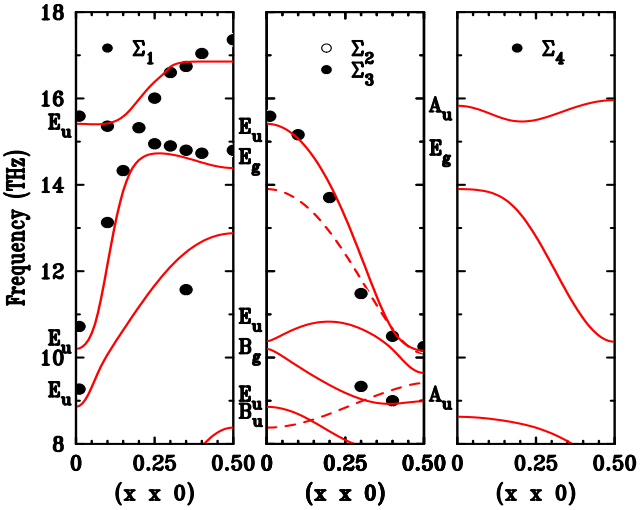

FIG. 10: Dispersion of the high-energy phonon branches in $Nd_{1.85}Ce_{0.15}CuO_4$ in [110] direction. Symbols denote measured frequencies and lines results of the lattics dynamical calculations (the broken line in the middle corresponds to the Σ_2 representation.

associated with Nd-O2 vibrations disperses steeply upwards from its starting point at $\nu = 9.4$ THz and becomes the highest one in frequency for **q** larger than (0.15 0.15 0). At the zone boundary it reaches a frequency of 17.4 THz, the highest in the entire dispersion. Raman experiments have observed a peak at just this frequency [39] suggesting that it should be attributed to the (0.5 0.5 0) LO O2-mode. This mode, which is not Raman active, may become so through the disorder induced by the Ce-doping. However, it remains astonishing that this disorder induced Raman-peak is that strong. In contrast to the Nd-O2 branch, the Cu-O1-bond-stretching branch is found to exhibit a downward dispersion similar to the observation along the [100] direction. However, the downward dispersion is less pronounced along [110] and has a more conventional shape, i.e. it is sine-like.

The transverse Cu-O1-bond-stretching branch of Σ_3-symmetry also exhibits a steep frequency decrease when passing into the Brillouin-zone, see the right part of Fig. 9 and Fig. 10. The transverse bond-stretching branch along the [110] direction ends at the zone-boundary in the so-called quadrupolar mode, whose polarization pattern is given in Fig. 1. Its low frequency compared to that of the zone centre mode is perfectly described by the lattice dynamical model without any need for a special force constant. The shape of this branch has to be considered as normal. A similar shape is observed in many other perovskites. The relatively low frequency of the quadrupolar mode can be understood from the fact that this vibration involves weaker force constants compared to the zone center bond-stretching mode, as the O1-O1 distances vary only little.

IV. Discussion of bond-stretching phonon anomalies

– *Comparision with inelastic x-ray scattering data* – Qualitatively, our results agree with the anticrossing scenario of Cu-O1 bond-stretching and Nd-O2 modes which was deduced from an inelastic x-ray experiment [24, 25], but quantitatively, there are significant differences for **q**-values away from the Brilluoin-zone center. For the [100] direction we find good agreement up to **q**=(0.15 0 0), whereas already at **q**=(0.2 0 0) the tentative identification of the bond-stretching mode near 12 THz seems to be incorrect, see Fig. 11 . The inelastic x-ray spectra are dominated by the contribution of the Nd-O2 peak, therefore, the bond-stretching frequencies could not be determined unambiguously but had to be fitted to the little structured back ground. For instance, inspection of Fig. 2 in [24] shows that no clear peak was observed at the position of the Cu-O1 mode for **q**=(0.4 0 0). The approximate agreement between the x-ray and the neutron frequencies for this **q** appears to be somewhat accidental.

The problems encountered in the x-ray experiment aiming at the dispersion of the Cu-O1 bond-stretching modes in the [110] direction are similar to those just discussed for the [100] direction. In particular, the inelastic structure factors of these modes are very small for **q** beyond (0.25,0.25,0) in the Brillouin zone chosen for the measurements. Therefore, it is not surprising that the

x-ray data for this q-region are quite inaccurate and fall 1.5 THz below the neutron data.

In summary, our neutron results confirm the anti-crossing scenario discussed in [24, 25] but only qualitatively so. The neutron experiment is much better suited to resolve the complex multi-branch dispersion by examining many different Brillouin zones and due to the fact that oxygen and heavy-ion modes posses similar dynamical structure factors for neutron scattering. Higher order scattering events may play a stronger role in the case of inelastic x-ray scattering studies on the oxygen modes.

– *Comparision of bond-stretching phonon anomalies in high temperature superconductors* – Due to the mixing of several branches in $Nd_{1.85}Ce_{0.15}CuO_4$ it is not obvious to isolate the behavior of the bond-stretching modes in the [100] direction from Fig. 5. Therefore, we present the Δ_1- data again in Fig. 11, where the frequencies of the modes with bond-stretching character are drawn as filled and all other contributions as open circles, respectively. The separation can be easily done in the first half of the Brillouin-zone, but is less obvious in the second half due to the interaction with the *c*-polarized modes, which is more extended in **q**-space. The presentation in Fig. 11 clearly shows the resemblance of the bond-stretching dispersion in $Nd_{1.85}Ce_{0.15}CuO_4$ with that in $La_{1.85}Sr_{0.15}CuO_4$ [11]. The observed dispersion is rather well reproduced by the shell model after inclusion of the additional breathing constants except that the frequency drop around **q**= (0.25,0,0) is sharper in experiment . We emphasize that the classical shell model without such force-constants predicts an upwards bond-stretching dispersion as is indicated in Fig. 11 by broken lines. In the top of Fig. 11 we show the differences between the measured bond-stretching frequencies and those calculated from the shell model without breathing constants. These differences demonstrate the influence of the anomalous strong electron-phonon coupling in $Nd_{2-x}Ce_xCuO_4$.

The anomalous bond-stretching dispersion in $Nd_{1.85}Ce_{0.15}CuO_4$ is compared with that of other cuprate superconductors in Fig. 12. Evidently, the dispersion in the [100] direction is step-like in all optimally doped cuprate superconductors investigated so far. The different levels of bond-stretching phonon frequencies can be attributed to different Cu-O1-bond distances induced either through different dopants or through internal strain. When comparing the frequencies of the half-breathing mode to those of the zone-centre bond-stretching mode we find the strongest renormalisation in the two high-T_c materials $YBa_2Cu_3O_7$ and $HgBa_2CuO_4$; $La_{1.85}Sr_{0.15}CuO_4$ exhibits a slightly stronger softening than $Nd_{1.85}Ce_{0.15}CuO_4$ along [100] [43]. In contrast, the downward dispersion along the [110] direction is most pronounced in $Nd_{1.85}Ce_{0.15}CuO_4$whereas the corresponding branch in $La_{1.85}Sr_{0.15}CuO_4$ is nearly flat and exhibits even a weak frequency increase in $YBa_2Cu_3O_7$ [10]. That is to say, $Nd_{1.85}Ce_{0.15}CuO_4$ shows the least anisotropy between the frequency renormalisation along the [100] and the [110] directions of all optimally doped cuprates studied so far. In this sense, it can be said that the phonon softening in $Nd_{1.85}Ce_{0.15}CuO_4$ has the least one-dimensional character. It remains to be seen whether this fact is related to the distinct character of the charge carriers, electron versus hole-like, in the cuprate high-temperature superconductors. It is worth mentioning that the one-dimensional nature of the over-screening effect is most pronounced in the 90 K-superconductor $YBa_2Cu_3O_6$. But we want to emphasize once more, that the anomalous bond-stretching phonon dispersion in all superconducting cuprates is astonishingly similar.

There is an on-going debate about the importance of electron phonon coupling for the kink-like features observed in ARPES spectra of many cuprate high temperature superconductors [2, 3, 44]. However, there seem to be significant differences between the ARPES features of hole and electron doped compounds [45], whereas we find the phonon anomalies in the bond-stretching branches in all cuprates to be essentially the same. This raises doubts about a dominant role of the bond-stretching modes for the ARPES features.

–*Comparison with other metallic perovskites* – The over-screening effects in the bond-stretching dispersion are not a particularity of the superconducting cuprates but are seen in many doped perovskites : nickelates [16, 17], manganates [18] and superconducting $Ba_{1-x}K_xBiO_3$ [19, 20, 21], the only metallic perovskite compound which does not exhibit the effect is superconducting Sr_2RuO_4 [22], allthough this material is the best metal. The frequency softening is even much more pronounced in manganates and bismuthates than in the cuprates [21].

Fig. 12 further demonstrates that many perovskite materials exhibit even a similar shape of the bond-stretching dispersion along [100]. The step-like shape of the dispersion is observed in $Ba_{1-x}K_xBiO_3$ and in $La_{1-x}Sr_xMnO_3$ for x=0.2 and 0.3 . In the nickelates, however, the dispersion is nearly sinusoidal. This dispersion may be related to the insulating electronic behavior in nickelates [21, 46]. The absolute size of the over-screening effects differs essentially between the systems. The effect along [100] is strongest in the manganates where it amounts to a reduction by 30% . Along the other directions in reciprocal space, the manganates and $Ba_{1-x}K_xBiO_3$ exhibit over-screening effects which even exceed those occurring along [100]. For instance, the volume breathing mode in $Ba_{1-x}K_xBiO_3$ is renormalized by 40% compared to the insulating reference material [20, 21]. A strong softening in the [110] direction was observed also in the nickelates. This indicates that the electron-lattice coupling is quite strong in these materials, even considerably stronger than in the cuprates. This conclusion is corroborated by the fact that in the manganites and in $Ba_{1-x}K_xBiO_3$ the phonon anomalies

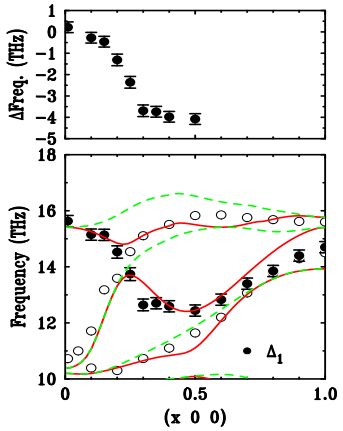

FIG. 11: (Below) Dispersion of the bond-stretching phonon frequencies (filled circles) and other modes (open circles) compared to the calculated phonon frequencies. The dashed and continous lines correspond to screened shell-model calculations without and with the additional breathing-force constants, respectively. (Above) Difference between the measured bond-stretching frequencies and the shell-model calculations without the breathing forces.

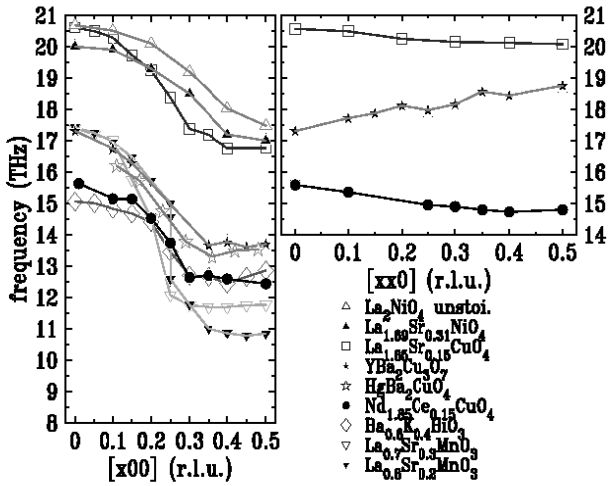

FIG. 12: Comparison of the phonon anomaly in the bond-stretching branches observed in different metallic oxide perovskite materials. In the left we show the dispersion along the [100] direction and in the right part that for the [110] direction. Data were taken from references : Unstoichiometric La_2NiO_4 [16], $La_{1.69}Sr_{0.31}NiO_4$ [17], $La_{1.85}Sr_{0.15}CuO_4$ [11], $YBa_2Cu_3O_6$ [13], $HgBa_2CuO_4$ [26], $Ba_{1-x}K_xBiO_3$ [19], and $La_{1-x}Sr_xMnO_3$ [18].

are not restricted to a line in reciprocal space but are very strong also in other directions. Therefore, they entail a much stronger shift of spectral weight in the PDOS.

We think that there is a close relationship of the bond-stretching phonon anomalies with the charge ordering phenomena in each particular system [21]. All these systems including the cuprates are close to charge ordering instabilities, which may be stabilized by a particular doping [46, 47, 48]. Roughly speaking, those bond-stretching modes are most renormalized in frequency whose polarization patterns corresponds to the structural distortion induced by the charge ordering. The most obvious difference between the cuprates and other perovskite compounds consists in the fact that the [100] direction plays a special role only in the cuprates, what perfectly reflects the one-dimensional nature of charge ordering in the form of stripes in hole-doped cuprates. In contrast, charge ordering phenomena in nickelates, manganates and bismuthates occur with a checker-board arrangement. Concurrently, the strongest bond-stretching phonon anomalies in these compounds occur along the related [110] or [111]-directions. The relation between charge ordering and bond-stretching phonon anomalies also holds for the ruthenate, since in layered ruthenates, which exhibit a normal bond-stretching phonon dispersion, in-plane charge ordering seems not to occur.

Charge ordering phenomena have so far not been observed in the electron-doped cuprates. From their similar phonon dispersion, one may expect them to appear most likely again along the [100]-direction.

Anomalous peak splitting has been reported for a number of perovskite materials and have been taken as fingerprints of an inhomogeneous charge distribution, i.e. in $Ba_{1-x}K_xBiO_3$ [20, 21], in the nickelates [17], and also in $YBa_2Cu_3O_6$ and $La_{1.85}Sr_{0.15}CuO_4$ [12, 14]. For the latter two materials, however, it was shown that there are no indications for intrinsic splittings of bond-stretching branches [11, 15]. We note that in $Nd_{1.85}Ce_{0.15}CuO_4$ as well, all observed peak splittings of bond-stretching phonons can be fully explained with standard theory of lattice dynamics, i.e. due to the interaction of branches having the same symmetry.

IV. CONCLUSION

Inelastic neutron scattering allowed us to quantitatively characterize the high-energy phonon dispersion in $Nd_{1.85}Ce_{0.15}CuO_4$. Previous inelastic x-ray measurements had already shown that the frequencies of the Cu-O bond-stretching branches are strongly renormalized when compared to those of the insulating parent compounds but reliable data could be obtained only for a limited range of wave vectors very close to the zone center whereas the frequencies of the linear and of the planar breathing modes were not accessible.

The dispersion of the branches with Cu-O1 bond-stretching character exhibits anomalies astonishingly similar to the observations in hole doped cuprate superconductors. Along the [100] direction the frequency of the bond-stretching modes abruptly decreases near $\mathbf{q}$=(0.25 0 0). This effect is slightly weaker than in the hole doped materials. Moreover, these phonons acquire

a large linewidth which underpins their anomalous character. The longitudinal bond-stretching modes exhibit a downward dispersion also along the [110] direction with a frequency drop between zone center and zone boundary of about 1 THz but the dispersion shape of the branch appears to be more normal. The softening of the planar breathing-mode softening in $Nd_{1.85}Ce_{0.15}CuO_4$ is stronger than the corresponding effect in the hole doped materials, in particular compared to $YBa_2Cu_3O_6$, indicating that the anomalous softening of the linear breathing mode has weaker one-dimensional character. However, the differences in the phonon anomalies between hole and electron doped cuprates concern details; the signatures of electron phonon coupling in the bond-stretching phonons are found to be essentially the same in all cuprate high temperature superconductors studied so far.

Acknowledgments This work was supported by the Deutsche Forschungsgemeinschaft through the Sonderforschungsbereich 608 and by the specific grants-in-aid from the MEXT (Japan). We acknowledge helpful discussions with M. d'Astuto.

* Electronic address: braden@ph2.uni-koeln.de

[1] P.W. Anderson, Physica Scripta T102, 10 (2002).
[2] Z.-X. Shen, A. Lanzara, S. Ishihara, and N. Nagaosa, Philos. Mag. B 82 1349 (2002).
[3] A. Lanzarra et al., Nature 412 510 (2001).
[4] C. Falter, cond-mat/0403564.
[5] M. Tachiki, M. Machida, and T. Egami Phys. Rev. B 67, 174506 (2003).
[6] W. Weber, Phys. Rev. B 8, 5093 (1973); C.M. Varma and R.C. Dynes in, Superconductivity in d- f-band metals, erdited by D.H. Douglass, Plenum, New York (1976).
[7] B. Renker et al., Z. Phys. 67 15 (1987); Z. Phys. 71 437 (1988); Z. Phys. 73 309 (1988).
[8] J.W. Lynn et al., et al., Phys. Rev. Lett. 66, 919 (1991).
[9] H.J. Kang et al., Phys. Rev. B 66, 064506 (2002).
[10] L. Pintschovius and W. Reichardt, in Neutron Scattering in Layered Copper-Oxide Superconductors, ed. by A. Furrer, Phys. and Chem. of Materials with Low-Dim. Structures, Vol. 20 (Kluwer Academic Publ., Dordrecht, 1998), 165.
[11] L. Pintschovius and M. Braden, Phys. Rev. B 60, R15039 (1999).
[12] R. J. McQueeney et al., Phys. Rev. Lett. 87 077001 (2001).
[13] W. Reichardt, J. Low Temp. Phys. 105, 807(1996).
[14] J.-H. Chung et al., Phys. Rev. B 67, 014517 (2003).
[15] L. Pintschovius, Y. Endoh, D. Reznik, H. Hiraka, J. M. Tranquada, W. Reichardt, H. Uchiyama , T. Masui and S. Tajima, Phys. Rev. B 69, 214506 (2004).
[16] L. Pintschovius, W. Reichardt, M. Braden, G. Dhalenne and A. Revcolevschi Phys. Rev. B 64, 094510 (2001).
[17] J. M. Tranquada, K. Nakajima, M. Braden, L. Pintschovius, and R. J. McQueeney Phys. Rev. Lett. 88, 075505 (2002).
[18] W. Reichardt and M. Braden, Physica B 263, 416 (1999).
[19] M. Braden et al., Europhysics Letters 34, 531 (1996).
[20] M. Braden, W. Reichardt, S. Shiryaev, and S.N. Barilo, cond-mat0107498 (2001).
[21] M. Braden, W. Reichardt, S. Shiryaev and S. Barilo, Physica C 378, 89 (2002).
[22] M. Braden, unpublished.
[23] N. Berg, SrTiO3 Diploma-thesis, Technische Hochschule Karlsruhe (1993).
[24] M. d'Astuto, P. K. Mang, P. Giura, A. Shukla, P. Ghigna, A. Mirone, M. Braden, M. Greven, M. Krisch, and F. Sette Phys. Rev. Lett. 88, 167002 (2002).
[25] M. d'Astuto et al., International Journal of modern Phys. B 17, 484 (2003).
[26] H. Uchiyama et al., Phys. Rev. Lett. 92, 197005 (2004).
[27] T. Fukuda, J. Mizuki, K. Ikeuchi, K. Yamada, A.Q. Baron, and S. Tsutsui, Phys. Rev. B 71, 060501 (2005).
[28] K. Yamada, K. Kurahashi, T. Uefuji, M. Fujita, S. Park, S.-H. Lee, and Y. Endoh, Phys. Rev. Lett. 90, 137004 (2003).
[29] M. Fujita, T. Kubo, S. Kuroshima, T. Uefuji, K. Kawashima, K. Yamada, I. Watanabe, and K. Nagamine Phys. Rev. B 67, 014514 (2003).
[30] I.D. Brown et al., Acta Cryst. B41, 244 (1985).
[31] G. H. Kwei, SW. Cheong, Z. Fisk, F. H. Garzon, J. A. Goldstone, and J. D. Thompson Phys. Rev. B 40, 9370-9373 (1989).
[32] S. L. Chaplot, W. Reichardt, L. Pintschovius, and N. Pyka Phys. Rev. B 52, 7230-7242 (1995).
[33] P. Brüesch, Phonons: Theory and Experiments (Springer-Verlag, Berlin, 1982), Vol. I. .
[34] We have chosen a large value of the linear breathing constant in order to describe the phonon dispersion but this value yields a shift of some breathing-mode character towards the next lowest branch. Nearly the complete bond-stretching character in $Nd_{1.85}Ce_{0.15}CuO_4$ at $\mathbf{q}$=(0.5,0,0) , however, appears to reside in the mode at 12.5THz.
[35] M. Tachiki and S. Takahashi, Phys. Rev. B 39, 293 (1989).
[36] C. Falter, M. Klenner, W. Ludwig, Phys. Rev. B 47, 5390 (1993).
[37] S. Y. Savrasov and O. K. Andersen, Phys. Rev. Lett. 77, 4430 (1996).
[38] K.P. Bohnen, R. Heid R, and M. Krauss, Europhys. Lett. 64, 104 (2003).
[39] E. T. Heyen, R. Liu, M. Cardona, S. Piol, R. J. Melville, D. McK. Paul, E. Morán, and M. A. AlarioFranco Phys. Rev. B 43, 2857-2865 (1991).
[40] E.T. Heyen, G. Kliche, W. Kress, W. König, M. Cardona, E. Rampf, J. Prade, U. Schröder, A.D. Kulkarini, F.W. de Wette, S. Pinol, D. McK.Paul, E. Moran and M.A. Alario-Franco, Sol. State Comm. 74, 1299 (1990).
[41] C. C. Homes, B. P. Clayman, J. L. Peng, and R. L. Greene Phys. Rev. B 56, 5525-5534 (1997).
[42] M. K. Crawford, G. Burns, G. V. Chandrashekhar, F. H. Dacol, W. E. Farneth, E. M. McCarron, III, and R. J. Smalley Phys. Rev. B 41, 8933-8936 (1990).
[43] In the case of $Nd_{2-x}Ce_xCuO_4$ it is difficult to directly compare undoped and doped compounds, because Cu-O1 bond-stretching modes are not pure in character in the undoped material but exhibit significant Nd-O2 character.
[44] S.V. Dordevic et al., cond-mat/0411043.
[45] N.P. Armitage et al., Phys. Rev. Lett 88,257001 (2002);

Phys. Rev. B 66, 064517 (2003).
[46] M. Imada, A. Fujimori, and Y. Tokura Rev. Mod. Phys. 70, 1039 (1998).
[47] B. J. Sternlieb, J. P. Hill, U. C. Wildgruber, G. M. Luke, B. Nachumi, Y. Moritomo, and Y. Tokura Phys. Rev. Lett. 76, 2169 (1996).
[48] P. G. Radaelli, D. E. Cox, M. Marezio, and SW. Cheong Phys. Rev. B 55, 3015 (1997).